

2



Lawrence Berkeley Laboratory

UNIVERSITY OF CALIFORNIA

RECEIVED
LAWRENCE
BERKELEY LABORATORY

Materials & Molecular Research Division

APR 17 1984

LIBRARY AND
DOCUMENTS SECTION

Presented at the 3rd Oxford Conference on Microscopy of Semiconducting Materials, Oxford, England, March 21-28, 1983; and published in the Proceedings

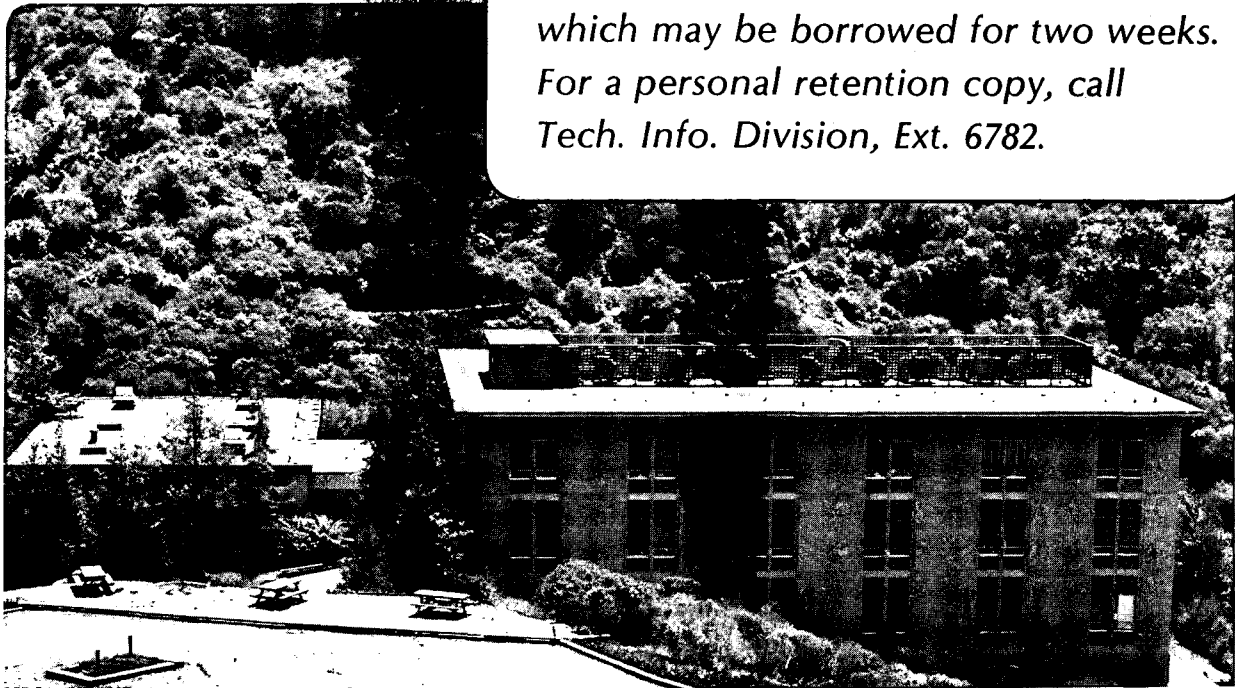
HEATPULSE ANNEALING OF ION-IMPLANTED SILICON:
STRUCTURAL CHARACTERIZATION BY TRANSMISSION
ELECTRON MICROSCOPY

D.K. Sadana, S.C. Shatas, and A. Gat

April 1983

TWO-WEEK LOAN COPY

*This is a Library Circulating Copy
which may be borrowed for two weeks.
For a personal retention copy, call
Tech. Info. Division, Ext. 6782.*



LBL-17320
ca

DISCLAIMER

This document was prepared as an account of work sponsored by the United States Government. While this document is believed to contain correct information, neither the United States Government nor any agency thereof, nor the Regents of the University of California, nor any of their employees, makes any warranty, express or implied, or assumes any legal responsibility for the accuracy, completeness, or usefulness of any information, apparatus, product, or process disclosed, or represents that its use would not infringe privately owned rights. Reference herein to any specific commercial product, process, or service by its trade name, trademark, manufacturer, or otherwise, does not necessarily constitute or imply its endorsement, recommendation, or favoring by the United States Government or any agency thereof, or the Regents of the University of California. The views and opinions of authors expressed herein do not necessarily state or reflect those of the United States Government or any agency thereof or the Regents of the University of California.

HEATPULSE ANNEALING OF ION-IMPLANTED SILICON: STRUCTURAL CHARACTERIZATION BY TRANSMISSION ELECTRON MICROSCOPY

D. K. Sadana, Lawrence Berkeley Laboratory, University of California, Berkeley, California

S. C. Shatas and A. Gat, AG Associates, Palo Alto, California

Abstract. A detailed structural investigation of Heatpulse rapid thermal annealed ion-implanted Si was carried out using TEM. Defect-free material was obtained after an 1100°C/10 sec. anneal for 80 KeV 2×10^{15} ^{75}As implanted Si, while dislocation loops were still present after lower temperature anneals. When compared with arsenic, 35 KeV ^{11}B implanted Si in the dose range 5×10^{14} exhibited markedly different behavior under the same annealing conditions, in that residual defects in the form of line dislocations, loops, and rods were observed. Comparison with 1000°C/30 min. furnace annealed samples showed differences in defect structures and impurity redistribution behavior as revealed by SIMS measurements. A model explaining the annealing behavior of implanted layers in silicon under rapid annealing conditions is proposed.

1. Introduction

Rapid annealing techniques employing incoherent light sources as an alternative to conventional furnace annealing of ion-implanted semiconductors have received a great deal of interest. Using arc lamps [1], graphite heaters [2], or tungsten-halogen lamps [3] as light sources and 1-100 second heating cycles, this technique offers similar advantages of scanned CW laser annealing: namely, high activation efficiency of the implanted species with minimal redistribution of the initial implanted profile [4]. Furthermore, the simplicity and energy efficiency of Heatpulse rapid thermal annealing compared with scanning laser or electron beam sources makes this process applicable to high volume manufacturing of integrated circuits. Extensive electrical measurements of rapid thermal annealed ion-implanted silicon have been reported [3,4], but studies of residual defects after annealing have so far been limited [6]. In this paper results of a detailed investigation of defect structures after Heatpulse annealing of boron and arsenic implanted silicon are presented.

2. Experimental

Czochralski grown (100) Si wafers, doped to a background concentration of $\sim 5 \times 10^{14} \text{ cm}^{-3}$ were implanted at room temperature in a non-channeling orientation. N-type phosphorous doped wafers were implanted with 35 KeV $^{11}\text{B}^+$ in doses of 5×10^{14} and $5 \times 10^{15} \text{ cm}^{-2}$, and p-type boron doped wafers were implanted with 80 KeV $^{75}\text{As}^+$ to a dose of $2 \times 10^{15} \text{ cm}^{-2}$.

Implanted samples were annealed in a Heatpulse apparatus, consisting of a water cooled reflective chamber containing upper and lower banks of tungsten halogen lamps. The stationary wafer, positioned equidistant between the lamp arrays, was rapidly heated at 50–100°C/sec. with up to 20 kW of radiant energy trapped between the reflectors. The lamp intensity, controlled by a microcomputer, was correlated with wafer temperature by using a type K thermocouple attached to the wafer. In a typical 1100°C, 10-second anneal cycle the lamp intensity was increased at a constant rate of 1.5 KW/sec., followed by a constant 76 percent intensity anneal of 10 seconds, and then decreasing the intensity at the same rate. The annealing ambient was air at atmospheric pressure, and a very small (<20Å) amount of oxide was grown during the anneal cycle. Samples furnace-annealed in a nitrogen ambient at 1000°C for 30 minutes served as a standard for comparison.

The implanted and annealed samples were then characterized by secondary ion mass spectrometry (SIMS) and TEM analysis. SIMS measurements were carried out with a Cameca IMS 3f ion microprobe analyzer using O_2^+ primary ion bombardment with positive ion detection for boron analysis. Sensitivity factors were obtained by integrating the as-implanted SIMS profile and equating this value to the implanted dose, and the depth scale for analysis was obtained by a Dektak measurement of the sputtered crater depth for each sample.

TEM analysis was performed on both plan view and cross-section specimens using bright-field diffraction conditions and micrographs were recorded for a (220) type diffraction vector.

Results

Figure 1a-c shows the TEM plan view micrographs from furnace and Heatpulse annealed Si samples that were implanted with boron to a dose of $5 \times 10^{14} \text{ cm}^{-2}$ at 35 KeV. All of the samples showed dislocation loops of $a/2 \langle 110 \rangle$ and $a/3 \langle 111 \rangle$ types. In addition, elongated rod and mix-

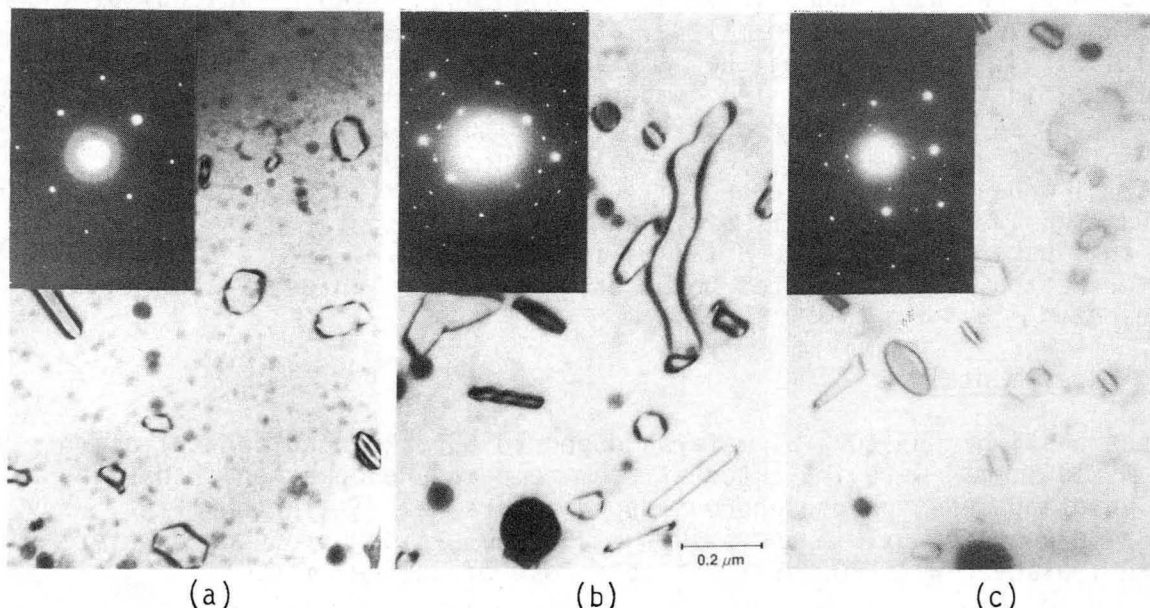


Fig. 1 TEM plan view micrographs of 35 KeV ^{11}B implanted (100) Si, $5 \times 10^{14} \text{ cm}^{-2}$; (a) furnace 1000°C/30 min. (b) Heatpulse 1100°C/10 sec. (c) Heatpulse 1100°C/30 sec. (XBB 833-2151)

shaped defects were present in the Heatpulse annealed samples. A large increase in the dimensions of the dislocation loops was observed when the Heatpulse annealing time was increased from 10 seconds to 30 seconds at 1100°C.

Figure 2a-d shows the annealing sequence for Si implanted with $5 \times 10^{15} \text{ cm}^{-2}$ B at 35 KeV. The as-implanted sample (Fig. 2a) exhibits a single-crystalline diffraction pattern, indicating that no amorphous layer is produced by the implanted boron even at this high dose. The furnace annealed sample (Fig. 2b) showed a high density of irregular shaped loops in addition to a dislocation network. In contrast, the sample Heatpulse annealed for 10 sec. (Fig 2c) showed the presence of a dislocation network still at its embryonic stage of formation. The extra spots in the diffraction pattern of this sample disappeared when thicker specimen foil areas were examined, giving no indication of the presence of polycrystalline Si in the implanted region. After a 30 sec. 1100°C Heatpulse anneal a well defined cross-grid dislocation network was observed to form in the implanted region (Fig. 2d).

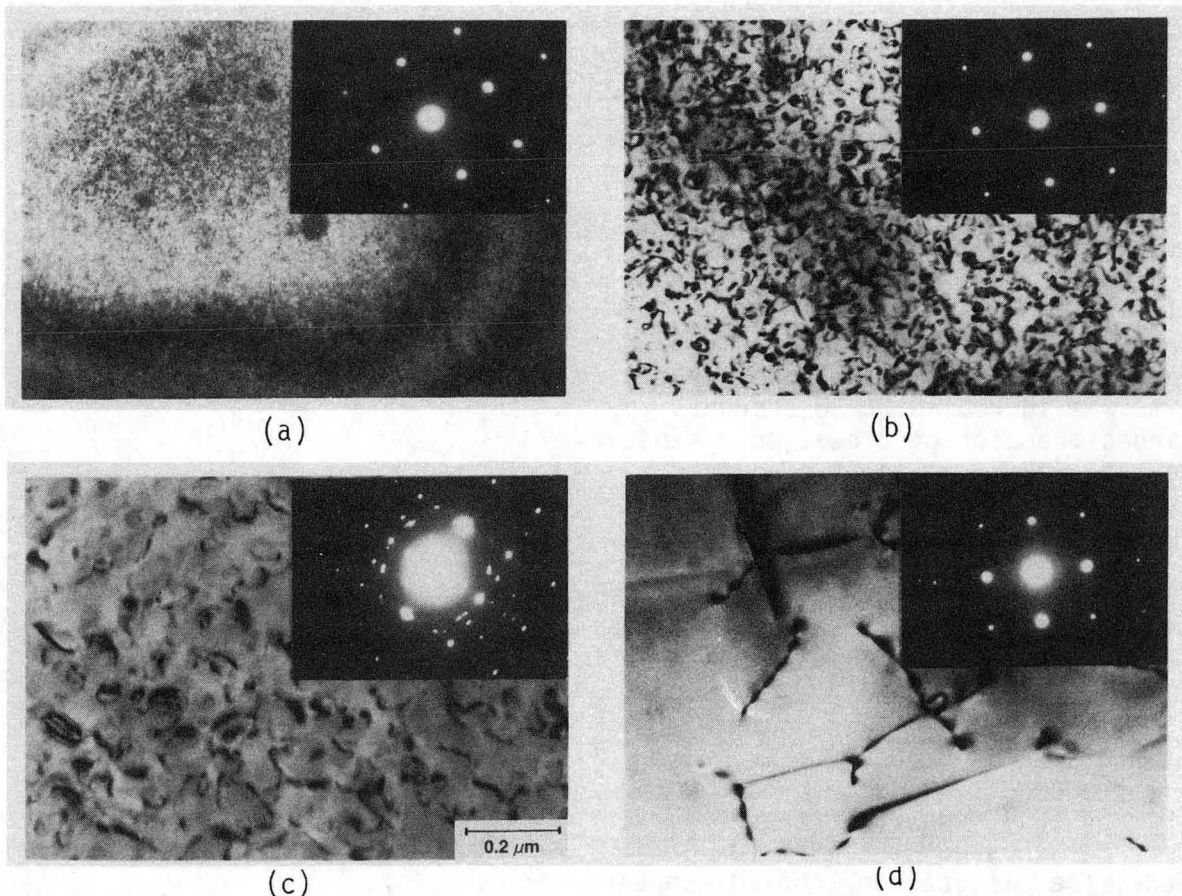


Fig. 2. TEM plan view micrographs of 35 KeV ^{11}B implanted (100) Si, $5 \times 10^{15} \text{ cm}^{-2}$; (a) as-implanted (b) furnace 1000°C/30 min. (c) Heatpulse 1100°C/10 sec. (d) Heatpulse 1100°C/30 sec. (XBB 833-2152)

The cross-section micrographs corresponding to Fig. 2a-c are shown in Fig. 3a-c. The as-implanted sample contained a $0.12 \mu\text{m}$ wide band of damage clusters at a mean depth of $0.09 \mu\text{m}$ from the surface. This depth

corresponds to 0.8 times the projected range (R_p) of $0.11 \mu\text{m}$ for boron at 35 KeV. Upon furnace annealing, the region containing damage clusters in Fig. 3b, converted into a dense band of dislocation loops (Fig. 3c). In addition, large loops and rods were found to be present below the initial damage layer that extended down to a depth of $0.38 \mu\text{m}$ from the surface. In contrast, the secondary defects in the Heatpulse annealed sample (Fig. 3a) were confined to a narrow band at a mean depth of $0.15 \mu\text{m}$ and did not show any deeply extending defects.

The SIMS profile of B from the as-implanted sample showed a characteristic skewed distribution (Fig. 3d). On subsequent furnace annealing broadening of the initial profile occurred with much bigger effect in the tail of the profile (Fig. 3d). Furthermore, pinning of B in the vicinity of R_p was observed. These results are in agreement with the earlier published results of Hofker [5]. The Heatpulse annealing for 10 seconds at 1100°C produced a B profile similar to that of above, however, the broadening in the tail region reduced markedly. When the Heatpulse annealing time was increased to 30 seconds, the pinned fraction of B near R_p disappeared and significant diffusion in the tail region comparable to that of the furnace annealed sample was observed.

In contrast to the annealing behavior of boron implanted silicon, Heatpulse annealing of arsenic implanted Si at 1100°C resulted in defect-free material (Fig. 4c). Dislocation loops with mean diameters of $0.04 \mu\text{m}$ remained after 1000°C 1-10 sec. anneals (Fig. 4a,b). When both these samples were re-annealed at 1100°C for 10 sec., the dislocation loops disappeared and defect-free material was once again obtained. Similar results have recently been reported for flame annealing of ion-implanted Si [6].

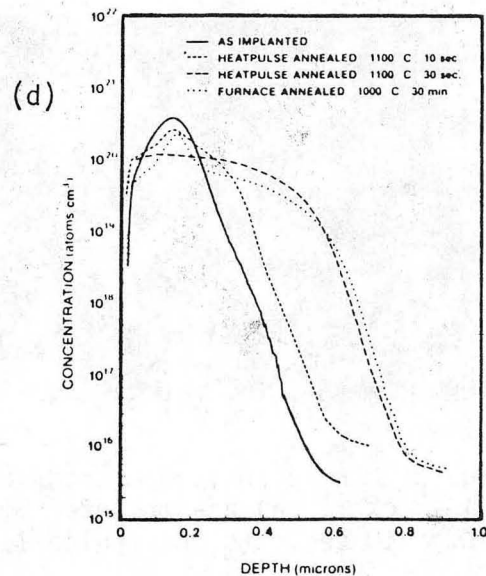
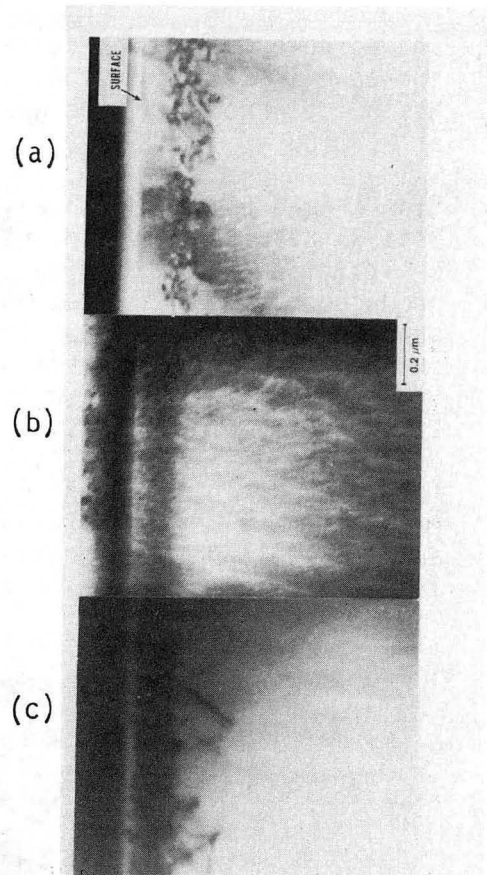


Fig. 3. Comparison of cross-section TEM micrographs corresponding to Fig. 2 with SIMS profiles of ^{11}B ; (a) Heatpulse $1100^\circ\text{C}/10 \text{ sec}$. (b) as-implanted (c) furnace $1000^\circ\text{C}/30 \text{ min}$. (d) ^{11}B SIMS profiles. (XBB 833-2150A)

Discussion

It appears from the results of Fig. 4 that perfection in recrystallization of the implanted region by Heatpulse annealing depends on the degree of amorphicity of the initial damage region and the annealing temperature. When the initial implant damage consists of a continuous amorphous layer that extend to the surface, as in the case of a high dose arsenic implant, the recrystallization on subsequent annealing can produce defect-free material. However, in the case of B where the initial damage structure consists of a high density of small damage clusters in the crystalline matrix, the recrystallization produces a high density of secondary defects. Impurities are known to play an important role in nucleation and stabilization of secondary defects [8]. They can segregate relatively easily to dislocations and be bound up with the dislocation core with some characteristic binding energy. At lower temperatures the impurities trapped at dislocations are not expected to escape and they retard the annealing out of the dislocations. Taking into consideration these factors, the results of Figs. 1-4 can be explained as follows. In the case of arsenic, when the Heatpulse annealing was carried out at 1000°C for 10 seconds, the amorphous layer is expected to recrystallize perfectly by solid phase epitaxial growth. The dislocation loops observed in the micrograph (Fig. 4a,b) probably correspond to the region just below the original amorphous/crystalline interface. If the As atoms in the vicinity of the loops segregate during the annealing process, the dislocations become pinned and their annealing will be retarded. At 1100°C, the binding energy of As to a dislocation is such that it is released from the core, thereby allowing complete annealing out of dislocation loops as observed in the 1100°C re-anneal of the samples initially annealed at 1000°C. Thus, defect-free material is obtained only after annealing at temperatures of 1100°C or higher.

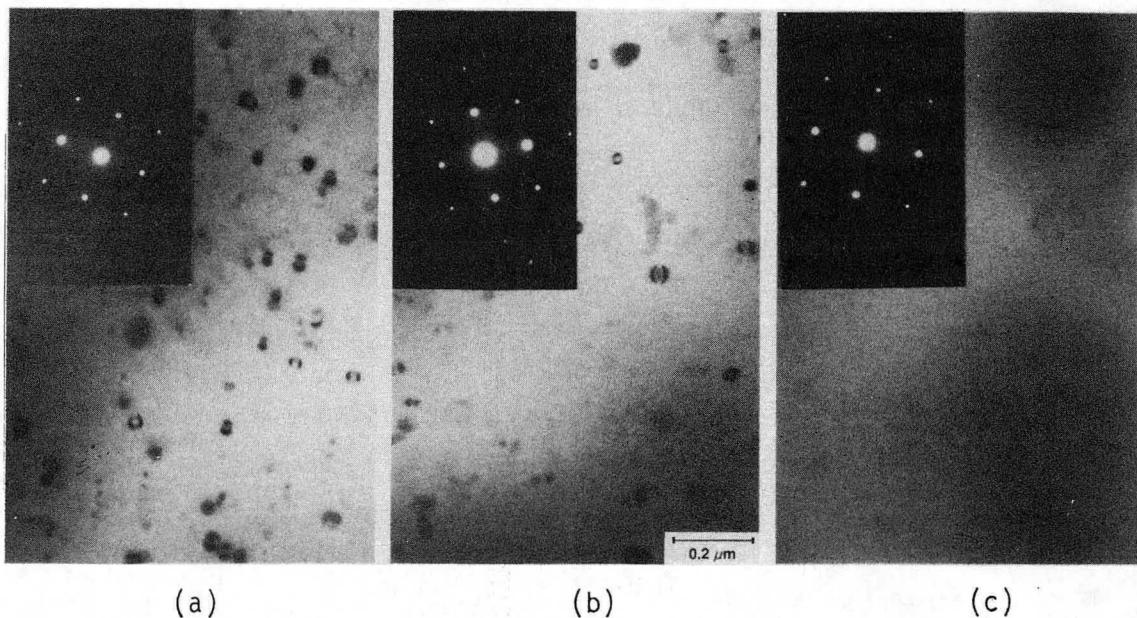


Fig. 4. TEM plan view micrographs of 80 KeV ^{75}As implanted (100) Si, $2 \times 10^{15} \text{cm}^{-2}$; (a) Heatpulse 1000°C/1 sec. (b) Heatpulse 1000°C/10 sec. and (c) Heatpulse 1100°C/10 sec. (XBB 833-2153)

In the case of boron implanted Si where the implant damage does not consist of an amorphous layer, the annealing process does not occur by simple solid phase epitaxial growth. However, the annealing behavior can still be explained qualitatively in a similar manner as that of arsenic implanted Si. Comparison of the cross-section TEM micrograph and B profile (Fig. 3) from the 1100°C/10 second sample shows that B segregates to the damage, but this segregation is less pronounced than that observed in the furnace annealed (1000°C/30 minutes) sample. When the Heatpulse annealing time was increased to 30 seconds, the segregated B atoms diffused away from the dislocations, allowing the loops to coarsen into a cross-grid dislocation network which does not anneal out. When the Heatpulse annealing was carried out in an argon ambient, defect-free material was observed after an 1100°C/10 second anneal for the 5×10^{14} cm⁻² boron implanted sample, in sharp contrast from the results shown in Fig. 1b. This difference in defect structure due to the annealing ambient may be explained by considering that the Si interstitials injected from the Si/SiO₂ interface during oxidation [7] can interact with defects already present and cause them to grow larger. Much longer diffusion lengths are observed in the Heatpulse annealed samples than is expected from the normal diffusion of B in Si. The cause of this enhanced diffusion during rapid thermal annealing is currently under investigation.

Acknowledgement

The authors would like to thank Professor Jack Washburn of the University of California, Berkeley, for useful discussions and Craig Hopkins of Charles Evans and Associates for the SIMS measurements. This work was supported by the Director, Office of Energy Sciences, Materials Research Division of the US Department of Energy under Contract No. DE-AC03-76SF00098.

References

1. Gat A 1981 IEEE Device Lett EDL-2(4) 85
2. Wilson SR, Gregory RB, Paulson WM, Hamdi AM and McDaniel FD 1982 App Phys Lett 41 978
3. Benton JL, Celler GK, Jacobson DC, Kimerling LC, Lischner DJ, Miller GL and Robinson McD 1982 Laser and Electron Beam Interaction with Solids ed BR Appleton and GK Celler (Elsevier, North Holland) pp 765-770
4. Benton JL, Celler GK, Jacobson DC, Kimerling LC, Lischner DJ, Miller GL and Robinson McD 1982 Laser and Electron Beam Interaction with Solids ed BR Appleton and GK Celler (Elsevier, North Holland) pp 771-776
5. Hofker WK 1975 Philips Res Rept Suppl 8
6. Narayan J and Young RT 1983 App Phys Lett 42 466
7. Lin AM, Antoniadis DA and Dutton RW 1981 J Electrochem Soc 128 1131
8. Sadana DK, Washburn J and Booker GR 1982 Phil Mag B 46 611

This report was done with support from the Department of Energy. Any conclusions or opinions expressed in this report represent solely those of the author(s) and not necessarily those of The Regents of the University of California, the Lawrence Berkeley Laboratory or the Department of Energy.

Reference to a company or product name does not imply approval or recommendation of the product by the University of California or the U.S. Department of Energy to the exclusion of others that may be suitable.

TECHNICAL INFORMATION DEPARTMENT
LAWRENCE BERKELEY LABORATORY
UNIVERSITY OF CALIFORNIA
BERKELEY, CALIFORNIA 94720